Influence of salt content on crack patterns formed through colloidal suspension desiccation

L. Pauchard, F. Parisse,* and C. Allain†
Laboratoire FAST, Unité Mixte de Recherche Paris VI, Paris XI, et CNRS, UMR 7608, Bâtiment 502, Campus Universitaire, 91405 Orsay Cedex, France
(Received 2 June 1998)

We analyze the influence of physicochemical properties on crack patterns formed by desiccation of a colloidal suspension, in the simple geometry of an isolated drop deposited on a flat surface. Depending on the suspension salinity, different types of crack patterns are observed: at low salinities a regular pattern of radial cracks develops all around the drop edge; at intermediate salinities, disordered patterns form, while at large salinities a unique circular crack appears. These behaviors are controlled by the evolution of the drop shape, that also depends on the suspension salt content. At intermediate salinities, large drop shape distortions appear that can be interpreted as a buckling instability. [S1063-651X(99)08903-5]

PACS number(s): 82.70.Dd, 62.20.Mk, 46.32.+x, 47.54.+r

In recent years, there has been a great deal of interest in fracture processes, and many works have analyzed the morphology of fracture surface and failure dynamics [1–3]. Few studies have dealt with cracking arising from the desiccation of complex fluids, although it is a widespread problem and a lot of diverse patterns have been observed [4–10]. Many phenomena of geological interest involve desiccation and cracking; these include muddy sediments in present day tidal flats or giant polygons in playa lakes [11]. On the other hand, many coating and material elaboration processes are based on the drying of colloidal suspensions; cracking and warping then generally need be avoided [12]. In the present paper, we experimentally study the influence of suspension salinity on the first stages of crack pattern formation.

The experiments are carried out on silica sols with well-controlled physicochemical properties in the simple geometry of an isolated drop deposited onto a flat surface. Depending on the suspension salinity, different crack patterns are observed: at low salinities a regular pattern of radial cracks builds up all around the drop edge [10,13], at large salinities a unique circular crack propagates, and for intermediate salinities a disordered pattern appears. We find that the difference between these behaviors is related to the evolution of the drop shape, which depends on the suspension salt content on the one hand, and on the competition between desiccation and gelation kinetics on the other hand [14]. The analysis of our experimental observations will be based on comparisons between the different characteristic times involved.

In the absence of evaporation, the stability of an aqueous colloidal suspension is governed by the interparticle colloidal interaction, i.e., by the competition between van der Waals attraction and electrostatic repulsion. Increasing the suspension salt content screens out the electrostatic interaction, and, depending on the particle volume fraction, flocculation or gelation of the suspension may occur. The experiments were performed with a volume fraction equal to 0.20; thus salt addition always leads to the formation of a gel. The suspensions are aqueous silica sols; the particle radius is 15 ± 2 nm. The pH is about 9.0, and so the particle surface bears a high negative charge density and DLVO theory is expected to apply [15]. The ionic strength value I was adjusted between 0.04 and 0.6 mol/l. To characterize the gelation kinetics of our samples, we performed rheological measurements. The results are well described by the scalar percolation model of the sol-gel transition [14]. The gelation time t_G is defined as the time elapsed after sample preparation when the zero shear steady state viscosity diverges. As displayed in Fig. 1, t_G strongly depends on I: for $I \leqslant 0.2$ mol/l, t_G is very long (larger than a day), while for $I \geqslant 0.4$ mol/l gelation occurs almost instantaneously (t_G is smaller than 100 s). For intermediate values of I, t_G exhibits a strong decrease with I due to the incomplete screening of the electrostatic repulsion i.e., to a colloidal interaction barrier which strongly decreases as I increases. Thus varying the suspension salt content allows one to vary the gelation time over an extended range of values. When solvent evaporation occurs, the ionic species and the particles accumulate, locally modifying the gelation time. However, it must be noted that the local values of the ionic strength and particle volume fraction can never be smaller than their initial values; thus t_G represents an upper bound for the gelation time for suspensions under desiccation.

The desiccation geometry used in the experiments is that of a drop deposited on a horizontal plate. Following water loss, contrasting with the case of a water drop that recedes with a constant contact angle, a drop of suspension recedes with a constant contact area. Indeed, as soon as evaporation begins, particles deposit onto the substrate, resulting in a strong anchoring of the three-phase line. Later on, the drop shape does not remain that of a spherical cap as for a pure water drop, large distortions appear which depend on the suspension ionic strength [14]. These shape distortions result from an inhomogeneous distribution of the particles, and on ionic species induced by water evaporation and from related changes in the mechanical properties.

*Electronic address: francois.parisse@fr.ibm.com
†Author to whom correspondence should be addressed. Electronic address: allain@fast.fast.u-psud.fr

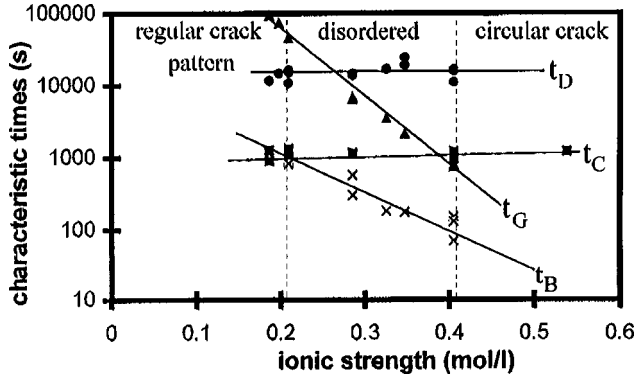

FIG. 1. Variations of the characteristic times with the suspension ionic strength (semilogarithmic scale): (▲) gelation time; (●) desiccation time; (■) first crack formation; (×) beginning of the buckling instability. Lines are solely to guide the eye. The dashed lines show three regions: a regular crack pattern, a disordered crack pattern, and a circular crack of a whole gelled drop.

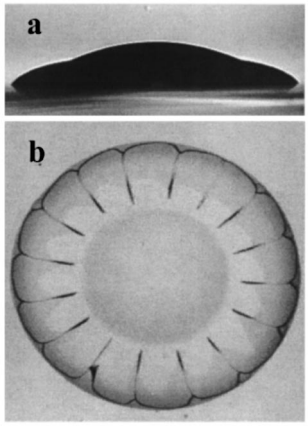

FIG. 2. (a) Side view: digitalized image of a colloidal suspension drop taken 15 min after deposition on a glass microscope slide. The ionic strength is equal to 0.04 mol/l. The initial contact angle is 40°, and the drop base diameter is 4 mm. A solid gelled foot builds up near the drop edge, while the central part remains fluid. (b) Top view: same drop taken 20 min after deposition. A regular pattern of radial cracks appeared all around the drop periphery, while the central part of the drop is still fluid.

Drop profiles and crack pattern formation were investigated using video recordings and image analysis. Our optical setup allowed us to obtain side and top views of the drop simultaneously. As previously reported, great care was taken to avoid optical distortions, in order to obtain the drop profile variation accurately [16]. The setup is placed inside a glove box (1.5 m^3) with the relative humidity (RH) controlled by a variable flow of nitrogen bubbling in a water bath. The flow is stopped before the beginning of the desiccation experiment to prevent any convection inside the box. All experiments were performed with a RH of 55% and an initial drop volume V_0 equal to 5 mm^3. The substrate is a carefully cleaned microscope glass slide. It should be noted that, since cracks nucleate at the later line, it is important to avoid defects of the three-phase line (dust, wetting defects, etc.). In the experiments reported here, only one crack nucleates: the observed patterns are developed by successive branching starting from this first crack. The contact angle (measured just after drop deposition) is found to be constant, independent of I: $\theta \cong 40°$. In order to characterize desiccation kinetics, we introduce the time $t_D = R_0/\omega_E$ where R_0 is the drop base radius (which remains constant during desiccation) and ω_E is the mean water flux per unit surface computed from profile recording ($\omega_E = -S^{-1}dV/dt$, where S and V, respectively, are the surface and volume of the drop at time t). In our experimental situations, evaporation is limited by diffusion of water into air: thus the only length scale involved is the drop size, which allows one to write desiccation characteristic time as R_0/ω_E. For a water drop, under the same conditions, t_D gives the order of magnitude of the time needed for a complete evaporation of the drop. For a colloidal suspension drop, ω_E is expected to be close to the value of ω_E for water, at least as long as the air/water meniscus has not receded inside the gel and the ionic strength is not too large [12]. This corresponds well to our observations: ω_E is found to be independent of time and of I in the range of volume variations investigated: $\Delta V/V_0 \leqslant 30\%$. Figure 1 displays the variation of t_D with I. Finally, it is to be noted that, in all the experiments, the suspension sample was prepared just before drop deposition; thus desiccation and gelation always begin simultaneously. Let us now describe different shape sequences and crack patterns observed depending on the ionic strength. Three types of behaviors can be distinguished that are considered successively in the following.

At low ionic strengths ($I \leqslant 0.18$ mol/l), the gelation time is larger than the desiccation time: typically, $t_G/t_D > 100$ (see Fig. 1). As previously reported [10,16] particles and ionic species then accumulate near the three-phase line, leading to the formation of a gelled ''foot,'' whereas the central part of the drop remains fluid [see Fig. 2(a)]. The mechanism responsible for foot formation [10,16] is similar as in the colloidal rings appearing during drying that were recently studied by Deegan *et al.* [17]; however, in contrast to our case, the starting volume fraction they used was very small (close to 10^{-4}), and, under their physicochemical conditions, gelation does not occur. As desiccation goes on, the foot extent increases, while the fluid central part shrinks regularly. Furthermore, under solvent evaporation, the gelled foot tends to shrink, and large stresses appear. These stresses are mainly orthoradial, since the central part of the drop is still fluid and the gelled foot behaves as a ring adhering onto the substrate. As time increases, the stresses increase until a certain time t_C at which their intensity becomes large enough to nucleate a first crack starting from the three-phase line. During the following 60 s later, a pattern of regularly spaced cracks builds up all around the drop edge [see Fig. 2(b)]. The observed periodicity comes from the coupling between stress relaxation and evaporation [9,13]. This type of behavior (gelled foot formation and regular crack pattern) is observed for I smaller than 0.18 mol/l. t_G is then always larger than t_D. Time t_C, at which the first crack forms, is found to be independent of the ionic strength (see Fig. 1). As expected, t_C is smaller than t_D ($t_C/t_D \cong 0.1$), since cracking begins before complete desiccation. In the same manner, t_C is smaller than t_G: the first crack forms before gelation had occurred in the whole drop. This is required to observe radial cracks since the drop central part must still be fluid.

At intermediate ionic strengths (0.18 mol/l $\leqslant I \leqslant$ 0.4 mol/l), gelation and desiccation times are of the same order; typi-

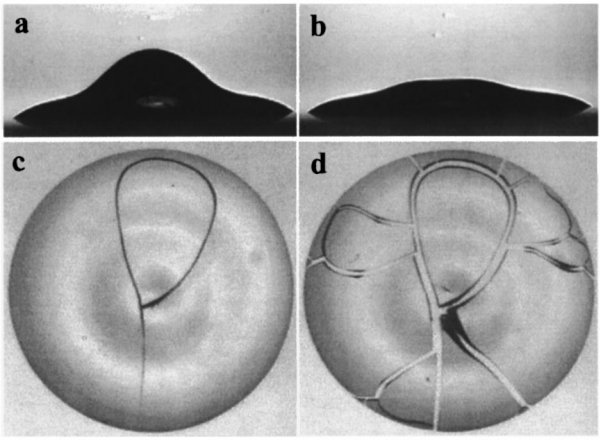

FIG. 3. (a) and (b) Side views of a drop taken 15 (a) and 20 min (b) after deposition. The ionic strength is equal to 0.285 mol/l. The initial contact angle is 38°, and the drop base diameter 4 mm. As time passes, the apex height, after a first decrease, begins to increase, reaches a maximum value that can be larger than its initial value, and finally decreases again. (c) and (d) Top views of the same drop taken 20 (c) and 22 min (d) after deposition. The first formed crack propagates through the drop center since a solid gelled skin had developed (c). A few tens of seconds later, a disordered pattern of cracks forms.

cally, t_G/t_D ranges from 10^{-1} to 10. At short times, the drop shape evolution is the same as described before. A gelled foot forms near the three-phase line, while the central part of the drop remains fluid. As time goes on, the central part progressively recedes until time t_B. At that time, the shape evolution changes: the foot stops widening and large distortions of the central part occur [see Figs. 3(a) and 3(b)]. In particular, the height of the apex stops decreasing, and then increases toward a maximum value before decreasing again. After time t_B, the simple test of sucking up the drop shows that the drop surface is solid. However, the inside of the central part has not gelled, since such large distortions could not occur in a completely gelled drop; thus t_B has to be smaller than t_G. The observed evolution is due to a buckling instability. Under evaporation, the solvent flows through the solid gelled skin (a colloidal gel behaves as a porous medium allowing solvent transport), so the volume included inside the skin decreases while the skin surface remains constant. Note that the values measured for S and ω_E remain constant for $t \geqslant t_B$, showing that the air-water meniscus has not receded inside the gelled skin.

To characterize the dynamics of this buckling instability, we have realized spatiotemporal diagrams allowing recording the apex height as a function of time. Figure 4 displays the results obtained for several drops in the intermediate ionic strength regime, and for a reference one corresponding to a low ionic strength ($I = 0.04$ mol/l; $t_G/t_D > 100$). In these curves, the time t_B, which corresponding to the onset of the buckling instability, is defined as the time where the apex height variation first deviates from the standard behavior. As displayed in Fig. 1, t_B strongly decreases with I. For I smaller than 0.18 mol/l, the extrapolated value of t_B would be larger than t_C; practically, foot cracking and decohesion will occur before this buckling instability arises. For I larger than 0.4 mol/l, no large shape distortions have time to take

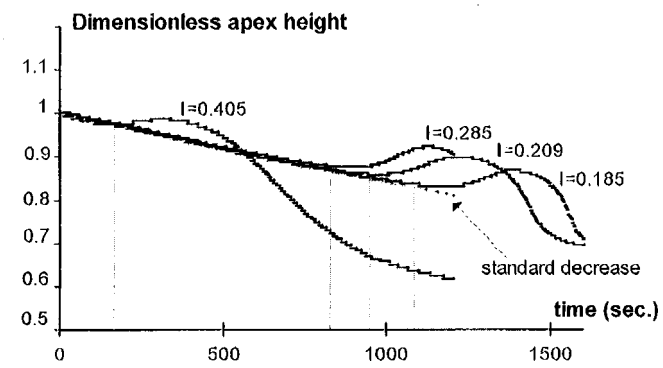

FIG. 4. Dimensionless apex height vs time for different ionic strengths: the standard decrease (0.040) and intermediate values (given in mol/l).

place, since the gel time is very short and t_B, if it exists, will be difficult to measure.

The formation of a gelled skin at the drop surface also influences cracking. In this range of ionic strengths, disordered patterns are observed. The first crack starts from the three-phase line and, as previously, propagates along a drop radius. However, in contrast to the case of small I where only the drop edge foot is gelled, the crack does not stop but passes through the drop center along a diameter before looping back [see Fig. 3(c)]. It is noted that the time necessary for this first crack to propagate is shorter than $\frac{1}{25}$ s. Later, after about 60 s, other cracks form, leading to a disordered pattern [see Fig. 3(d)]. Near the limit between small and intermediate I values ($I \cong 1.8$ mol/l), cracking initially begins as in the case of a regular pattern, but, after a certain time, the newly formed crack goes through the drop and stops the development of the regular pattern. At that time the surface of the central part has gelled, i.e., it can be cracked and buckling begins taking place ($t_C \cong t_B$). For I larger than 1.8 mol/l, t_B

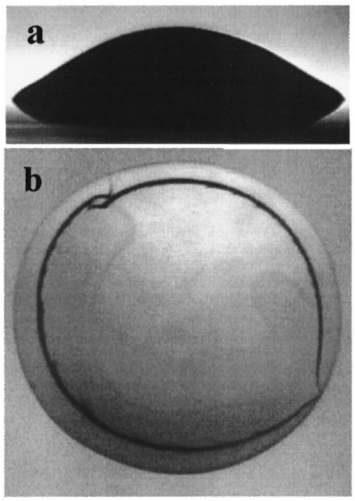

FIG. 5. (a) Side view of a drop taken 15 min after deposition for an ionic strength equal to 0.54 mol/l. The initial contact angle is 37°, and the drop base diameter is 4 mm. The gelation time is very short compared with desiccation time; the drop entirely gels. (b) Top view of the same drop taken 21 mm after deposition. Two cracks nucleate from the same point of the three-phase line, propagate in opposite directions, and then meet each other after covering half a circle.

is smaller than t_C and, depending on I, cracking occurs at different times with respect to the buckling instability (see Fig. 4). In all cases, the first crack propagates along a drop diameter and disordered crack pattern forms.

At large ionic strengths ($I \geqslant 0.4$ mol/l), the gelation time is shorter than the drying time (t_G/t_D smaller than 10^{-2}). The drop still recedes with a constant contact area, but now its shape does not change much during desiccation since the whole drop volume is gelled very quickly. However, the drop shape does not remain that of a spherical cap; a smooth inversion of the curvature is observed in the profile [see Fig. 5(a)]. This inversion may result from surface distortions taking place before complete gelation like the buckling instability observed in the intermediate range of I. At time t_C, a crack develops, starting, as previously, from the three-phase line; propagates along a circle near the drop edge; and stops just before crossing itself. In other cases, two cracks nucleate from the same point of the three-phase line, propagate in the opposite direction, and then join after covering half a circle each [see Fig. 5(b)]. In the range of ionic strengths considered, t_G is very small, and the stresses resulting from solvent loss are mainly radial, leading to an orthoradial crack propagation. Then secondary cracks form, but in contrast with the previous cases they appear later (typically several minutes later). As shown in Fig. 5(b), the pattern obtained at the first step of the cracking is a unique circular crack.

In summary, we find that the differences between the suspension ionic strengths (salt content) are responsible for the large variety of crack patterns induced by desiccation. Different regimes exist depending on the relative values of the characteristic times involved. The gelation time is very sensitive to the ionic strength, and following its value compared to the characteristic times of desiccation and crack beginning, three types of structures are found: a regular pattern of radial cracks when t_G is very large, a disordered pattern for intermediate values of the ionic strength, and a unique circular crack when t_G is the smallest characteristic time. These patterns can be well explained in relation to the evolution of the whole drop shape. In particular, we show that the disordered pattern observed at intermediate values of the ionic strength is related to the formation of a solid gelled skin, and to the subsequent buckling instability.

We gratefully thank C. Bastin for her help with the experiments. We also want to acknowledge J. C. Castaing, J. Hinch, J. P. Hulin, L. Limat, and H. Van Damme for fruitful discussions.

[1] *Statistical Models for the Fracture of Disordered Media*, edited by H. J. Herrmann and S. Roux (North-Holland, Amsterdam, 1990).
[2] *Disorder and Fracture*, edited by J. C. Charmet, S. Roux, and E. Guyon (Plenum, New York, 1990).
[3] E. Bouchaud, J. Phys.: Condens. Matter **9**, 4319 (1997).
[4] T. J. Garino, in *Better Ceramics Through Chemistry IV*, edited by B. J. J. Zelinsky, C. J. Brinker, D. E. Clark, and D. R. Ulrich, MRS Symposia Proceedings No. 180 (Materials Research Society, Pittsburgh, 1990), p. 497.
[5] A. Atkinson and R. M. Guppy, J. Mater. Sci. **26**, 3869 (1991).
[6] P. Meakin, Thin Solid Films **151**, 165 (1987).
[7] H. Colina, L. de Arcangelis, and S. Roux, Phys. Rev. B **48**, 3666 (1993).
[8] A. Groisman and E. Kaplan, Europhys. Lett. **25**, 415 (1994).
[9] C. Allain and L. Limat, Phys. Rev. Lett. **74**, 2981 (1995).
[10] F. Parisse and C. Allain, Phys. Fluids **8**, 9 (1996).
[11] P. S. Plummer and V. A. Gostin, J. Sed. Petrology **51**, 1147 (1981).
[12] C. J. Brinker and G. W. Scherer, in *Sol-Gel Science: the Physics and Chemistry of Sol Gel Processing* (Academic, San Diego, 1990).
[13] F. Parisse and C. Allain (unpublished).
[14] F. Parisse, C. Bastin, and C. Allain, in *Fluid Mechanics of Coating Processes*, edited by P. Bourgin, Second European Coating Symposium Proceedings No. 367 (Patrick Bourgin, Strasbourg, France, 1997).
[15] R. K. Iler, *The Chemistry of Silica* (Wiley, New York, 1979).
[16] F. Parisse and C. Allain, J. Phys. II **6**, 1111 (1997); Langmuir **13**, 3598 (1997).
[17] R. Deegan, O. Bakajin, T. F. Dupont, G. Huber, S. R. Nagel, and C. A. Witten, Nature (London) **383**, 827 (1997).